Frontiers of Information Technology & Electronic Engineering
www.jzus.zju.edu.cn; engineering.cae.cn; www.springerlink.com
ISSN 2095-9184 (print); ISSN 2095-9230 (online)
E-mail: jzus@zju.edu.cn

# Multi-UAV cooperative target tracking with bounded noise for connectivity preservation*

Rui ZHOU[1], Yu FENG[1], Bin DI[2], Jiang ZHAO[†‡1], Yan HU[1,3]

[1]*School of Automation Science and Electrical Engineering, Beihang University, Beijing 100191, China*

[2]*National Innovation Institute of Defense Technology, Academy of Military Sciences PLA China, Beijing 100171, China*

[3]*CETC Key Laboratory of Aerospace Information Applications, Shijiazhuang 050081, China*

[†]E-mail: jzhao@buaa.edu.cn

Received Nov. 12, 2019; Revision accepted Jan. 3, 2020; Crosschecked July 28, 2020

**Abstract:** We investigate cooperative target tracking of multiple unmanned aerial vehicles (UAVs) with a limited communication range. This is an integration of UAV motion control, target state estimation, and network topology control. We first present the communication topology and basic notations for network connectivity, and introduce the distributed Kalman consensus filter. Then, convergence and boundedness of the estimation errors using the filter are analyzed, and potential functions are proposed for communication link maintenance and collision avoidance. By taking stable target tracking into account, a distributed potential function based UAV motion controller is discussed. Since only the estimation of the target state rather than the state itself is available for UAV motion control and UAV motion can also affect the accuracy of state estimation, it is clear that the UAV motion control and target state estimation are coupled. Finally, the stability and convergence properties of the coupled system under bounded noise are analyzed in detail and demonstrated by simulations.

**Key words:** Multi-UAV cooperative target tracking; Network connectivity; Kalman consensus filter; Bounded noise; Connectivity preservation

https://doi.org/10.1631/FITEE.1900617 **CLC number:** TN953; TP391.41

## 1 Introduction

Cooperative target tracking of multiple unmanned aerial vehicles (UAVs) has received significant attention in recent years. It is believed that multiple UAVs can improve the estimation accuracy and tracking robustness in comparison with a single UAV (Kim et al., 2010; Yan et al., 2017). Multi-UAV organization, distributed estimation and information fusion methods, and UAV motion control and network connectivity are the main concerns in the multi-UAV cooperative target tracking problem (Stachura and Frew, 2011; Lim et al., 2013; Ma and Hovakimyan, 2013; Li et al., 2019).

For the state estimation problems over multiple UAVs, the corresponding results can be categorized according to whether a fusion center exists or not. Unfortunately, due to inevitable cost constraints, such a centralized approach might be infeasible as it requires significant resources. As such, an alternative approach called distributed state estimation has recently received much research attention. The main idea of the distributed algorithm is to decentralize the function of the fusion center by employing local estimators in each intelligent sensor, where each estimator uses the local information and messages from the neighboring nodes (rather than all the nodes) to

‡ Corresponding author

* Project supported by the National Natural Science Foundation of China (Nos. 61773031, 61573042, 61803009, and 61903084) and the Jiangsu Province Science Foundation for Youths, China (No. BK20180358)

ORCID: Rui ZHOU, https://orcid.org/0000-0003-2476-1130; Jiang ZHAO, https://orcid.org/0000-0002-9873-156X

generate an estimate (Liu QY et al., 2018).

Consensus-based distributed estimation algorithms emerged as the combination of consensus algorithms and traditional filters, especially the Kalman filter (Olfati-Saber, 2007a, 2009; Casbeer and Beard, 2009a, 2009b; Wang YT et al., 2013). Olfati-Saber (2007a, 2009) developed several similar distributed Kalman filters based on consensus algorithms and the Kalman filter. The convergence of the estimation errors without considering the noise has been proven, and comparison of the algorithms has also been made. The distributed information filter (Casbeer and Beard, 2009a, 2009b) can be seen as the dual form of the Kalman consensus filter. The distributed unscented information filter was developed by Wang YT et al. (2013) for coordinated tracking of the target with nonlinear dynamics in sensor networks.

In centralized methods, all nodes transmit the collected data to a centralized data processing center, and the center shares the data processing results and returns them to each node. Therefore, the computational complexity of the fusion center is high. In distributed methods, each node exchanges information with other nodes within the communication range. The nodes can generate their own networks according to the location and energy. The network topology can be dynamically adjusted with the number, location, and external environment of the nodes to achieve the effect of energy saving, fault tolerance, and a great reduction in computational complexity.

Each UAV in the network fuses others' information through multi-hop communication in multi-UAV cooperative target tracking, so it is crucial to preserve network connectivity. The communication topology in the sensor network can be represented by undirected graphs in general (Yu et al., 2019). The second smallest eigenvalue of the graph Laplacian ($\lambda_2$) is an important parameter for graph connectivity. Maximizing $\lambda_2$ will result in connectivity improvement (Kim and Mesbahi, 2006; Zavlanos and Pappas, 2007). $\lambda_2$ can also be estimated in a decentralized manner; hence, the global connectivity can be maintained using decentralized controllers (Yang et al., 2010).

Connectivity preservation is quite popular in the multi-agent flocking and formation control problem (Zavlanos et al., 2009; Kan et al., 2012; Wen et al., 2012). The potential function method is a fundamental way to prevent the original communication links from disconnecting (Ji and Egerstedt, 2007; Zavlanos and Pappas, 2008; Zavlanos et al., 2009, 2011; Ajorlou et al., 2010). Thus, local network connectivity can be maintained. A hybrid system, which is an integration of connectivity control in discrete space and motion control in continuous space, was investigated in Zavlanos and Pappas (2008) and Zavlanos et al. (2009). The artificial potential functions therein are used to maintain communication links and avoid collision. Proper potential functions can also drive multi-agent systems to achieve desired configurations and flocking behaviors (Olfati-Saber, 2006; Tanner et al., 2007; Kan et al., 2012).

In multi-UAV cooperative target tracking, appropriate motion of UAVs can increase the network's information about the target, and this is called information-driven motion control (Olfati-Saber, 2007b; Olfati-Saber and Jalalkamali, 2012). In turn, the information increase would also affect the UAV motion control. Coupled estimation and motion control framework and algorithms for mobile sensor network flocking were studied in Olfati-Saber and Jalalkamali (2012), where stability analysis of the coupled system was also presented. However, the filter and the coupled system were analyzed without taking the input noise into account, and the network connectivity was not considered explicitly.

In this study, we investigate the multi-UAV cooperative target tracking problem with a limited communication range under bounded noise. The distributed Kalman consensus filter is presented, and the boundedness of the estimation errors is analyzed. With the estimation of the target state, we design a potential function based distributed UAV controller that drives the network to track a mobile target and also ensures communication link maintenance and collision avoidance. The stability and convergence of the coupled estimation and motion control system are analyzed in detail. It shows that the network as a whole tracks the target stably, and the estimation converges under certain assumptions.

## 2 Communication topology and network connectivity

Consider a network of $N$ UAVs with integrated communication and sensing capabilities tracking a mobile target. Assume that two UAVs can

communicate with each other when the distance between them does not exceed $R$. Let $\boldsymbol{q}_i \in \mathbb{R}^m$ denote the position of the $i^{\text{th}}$ UAV and $\boldsymbol{q} = \text{col}(\boldsymbol{q}_i)$ the spatial configuration of the team.

Taking UAVs as vertices in the graph, the proximity graph $G(\boldsymbol{q}) = (V, E(\boldsymbol{q}))$ can be used to represent the communication topology. Here, $V$ is the set of vertices, and $E(\boldsymbol{q})$ is the set of edges defined as

$$E(\boldsymbol{q}) = \{(i,j) \in V \times V : \|\boldsymbol{q}_i - \boldsymbol{q}_j\| \le R, i \ne j\},$$

where $\|\cdot\|$ means the 2-norm. If $(i,j) \in E(\boldsymbol{q})$, then the $j^{\text{th}}$ vertex is adjacent to the $i^{\text{th}}$ vertex, also known as a neighbor of the $i^{\text{th}}$ vertex. Clearly, $G(\boldsymbol{q})$ is undirected. A path from the $i^{\text{th}}$ vertex to the $j^{\text{th}}$ vertex is a sequence of distinct vertices starting with the $i^{\text{th}}$ vertex and ending with the $j^{\text{th}}$ vertex, and the consecutive vertices are adjacent. The undirected graph $G = (V, E)$ is said to be connected if there exists a path between any two different vertices in $G$ (Godsil and Royle, 2001).

The Laplacian matrix of graph $G$ is defined as $\boldsymbol{L} = \boldsymbol{\Delta} - \boldsymbol{A}$, where $\boldsymbol{A} = [a_{ij}]$ denotes the adjacency matrix with elements $a_{ij} = 1$ if $(i,j) \in E$, and $a_{ij} = 0$, otherwise. $\boldsymbol{\Delta} = \text{diag}(\sigma_{ii})$ denotes the valency matrix with diagonal elements $\sigma_{ii} = \sum_{j=1}^{N} a_{ij}$. The following statements hold for the Laplacian matrix $\boldsymbol{L}$ (Godsil and Royle, 2001; Olfati-Saber, 2006):

1. $\boldsymbol{L}$ is positive semidefinite. Denote its eigenvalues as $\lambda_1 \le \lambda_2 \le \ldots \le \lambda_n$. The smallest eigenvalue $\lambda_1 = 0$ and $\boldsymbol{1}_N = (1, 1, \ldots, 1)^{\mathrm{T}}$ is the eigenvector associated with $\lambda_1$.

2. $\boldsymbol{z}^{\mathrm{T}}\boldsymbol{L}\boldsymbol{z} = \dfrac{1}{2}\sum_i \sum_j a_{ij}(z_j - z_i)^2, \boldsymbol{z} \in \mathbb{R}^N$.

3. If graph $G$ is connected, then the second smallest eigenvalue $\lambda_2(\boldsymbol{L}) > 0$. $\lambda_2(\boldsymbol{L})$ is also known as algebraic connectivity of graph $G$, and is often used to indicate the speed of convergence of a linear consensus protocol (Olfati-Saber, 2006).

## 3 Distributed Kalman consensus filter

Consider a mobile target with dynamics:

$$\dot{\boldsymbol{x}} = \boldsymbol{A}\boldsymbol{x} + \boldsymbol{B}\boldsymbol{\omega}, \tag{1}$$

where $\boldsymbol{A} \in \mathbb{R}^{n\times n}$, $\boldsymbol{B} \in \mathbb{R}^{n\times d}$, and $\boldsymbol{\omega}$ is the zero-mean white Gaussian noise satisfying

$$E[\boldsymbol{\omega}(t)\boldsymbol{\omega}^{\mathrm{T}}(\tau)] = \boldsymbol{Q}(t)\delta(t-\tau)$$

with $\delta(\cdot)$ the Dirac delta function.

The network of $N$ sensors tracks the state of the target collaboratively. The measurement model of the $i^{\text{th}}$ sensor is given by

$$\boldsymbol{z}_i = \boldsymbol{H}_i\boldsymbol{x} + \boldsymbol{\upsilon}_i, \tag{2}$$

where $\boldsymbol{H}_i \in \mathbb{R}^{l\times n}$ and $\boldsymbol{\upsilon}_i$ is the zero-mean white Gaussian noise satisfying

$$E(\boldsymbol{\upsilon}_i(t)\boldsymbol{\upsilon}_i^{\mathrm{T}}(\tau)) = \boldsymbol{R}_i(t)\delta(t-\tau).$$

Assume that the system described by Eqs. (1) and (2) is controllable and observable, and that the covariance matrices $\boldsymbol{Q}(t)$ and $\boldsymbol{R}_i(t)$ are finite.

Then, the distributed Kalman consensus filter is described as follows (Olfati-Saber, 2007a):

$$\dot{\hat{\boldsymbol{x}}}_i = \boldsymbol{A}\hat{\boldsymbol{x}}_i + \boldsymbol{K}_i(\boldsymbol{z}_i - \boldsymbol{H}_i\hat{\boldsymbol{x}}_i) + \gamma\boldsymbol{P}_i\sum_{j\in N_i}(\hat{\boldsymbol{x}}_j - \hat{\boldsymbol{x}}_i), \tag{3}$$

$$\boldsymbol{K}_i = \boldsymbol{P}_i\boldsymbol{H}_i^{\mathrm{T}}{\boldsymbol{R}_i}^{-1}, \gamma > 0, \tag{4}$$

$$\dot{\boldsymbol{P}}_i = \boldsymbol{A}\boldsymbol{P}_i + \boldsymbol{P}_i\boldsymbol{A}^{\mathrm{T}} + \boldsymbol{B}\boldsymbol{Q}\boldsymbol{B}^{\mathrm{T}} - \boldsymbol{P}_i\boldsymbol{H}_i^{\mathrm{T}}{\boldsymbol{R}_i}^{-1}\boldsymbol{H}_i\boldsymbol{P}_i, \tag{5}$$

where $\hat{\boldsymbol{x}}_i$ is the estimated state by the $i^{\text{th}}$ sensor and $\boldsymbol{K}_i$ denotes the gain matrix of the filter. Define $\boldsymbol{\eta}_i = \boldsymbol{x} - \hat{\boldsymbol{x}}_i$ as the estimation error of the $i^{\text{th}}$ sensor. $\boldsymbol{\eta} = \text{col}(\boldsymbol{\eta}_1, \boldsymbol{\eta}_2, \ldots, \boldsymbol{\eta}_N)$ denotes the collective estimation error.

**Assumption 1** There exists $\delta > 0$ such that $\boldsymbol{\Lambda} + 2\gamma\hat{\boldsymbol{L}} \ge \delta\boldsymbol{I}$, where $\boldsymbol{\Lambda} = \text{diag}(\boldsymbol{H}_i^{\mathrm{T}}\boldsymbol{R}_i^{-1}\boldsymbol{H}_i + \boldsymbol{P}_i^{-1}\boldsymbol{B}\boldsymbol{Q}\boldsymbol{B}^{\mathrm{T}}\boldsymbol{P}_i^{-1})$, $\hat{\boldsymbol{L}} = \boldsymbol{L} \otimes \boldsymbol{I}_n$, and $\boldsymbol{L}$ denotes the Laplacian matrix of the network.

If there exist constants $b_\omega$ and $b_\upsilon$ such that $\|\boldsymbol{\omega}\| \le b_\omega$ and $\|\boldsymbol{\upsilon}_i\| \le b_\upsilon$, the input and measurement noise is called bounded. Then we have the following proposition:

**Proposition 1** Consider a network of $N$ sensors tracking a mobile target collaboratively. The target dynamics and sensor measurement model are given in Eqs. (1) and (2), respectively. Each sensor adopts the distributed filter given in Eqs. (3)–(5). If Assumption 1 holds, the collective estimation error $\boldsymbol{\eta} = \text{col}(\boldsymbol{\eta}_1, \boldsymbol{\eta}_2, \ldots, \boldsymbol{\eta}_N)$ is bounded.

**Proof** Noting $\hat{\boldsymbol{x}}_j - \hat{\boldsymbol{x}}_i = \boldsymbol{\eta}_i - \boldsymbol{\eta}_j$, we have

$$\dot{\hat{\boldsymbol{x}}}_i = \boldsymbol{A}\hat{\boldsymbol{x}}_i + \boldsymbol{K}_i(\boldsymbol{z}_i - \boldsymbol{H}_i\hat{\boldsymbol{x}}_i) - \gamma\boldsymbol{P}_i\sum_{j\in N_i}(\boldsymbol{\eta}_j - \boldsymbol{\eta}_i)$$

and

$$\dot{\boldsymbol{\eta}}_i = (\boldsymbol{A} - \boldsymbol{K}_i\boldsymbol{H}_i)\boldsymbol{\eta}_i + \gamma\boldsymbol{P}_i\sum_{j\in N_i}(\boldsymbol{\eta}_j - \boldsymbol{\eta}_i) + \boldsymbol{\Gamma}_i\boldsymbol{\omega}_i, \tag{6}$$

where $\boldsymbol{\Gamma}_i = [\boldsymbol{B},\ \boldsymbol{K}_i]$ and $\boldsymbol{\omega}_i = \left[\boldsymbol{\omega}^{\mathrm{T}},\ \boldsymbol{\eta}_i^{\mathrm{T}}\right]^{\mathrm{T}}$.

Since the system described by Eqs. (1) and (2) is controllable and observable, there exist constants $\overline{p} > \underline{p} > 0$ such that $\overline{p}\boldsymbol{I} \leq \boldsymbol{P}_i \leq \underline{p}\boldsymbol{I}$ for any $i \leq N$ (Liu S and Zhang, 2011).

Consider the following candidate Lyapunov function:

$$V(\boldsymbol{\eta}) = \sum_{i=1}^{N} \boldsymbol{\eta}_i^{\mathrm{T}} \boldsymbol{P}_i^{-1} \boldsymbol{\eta}_i. \tag{7}$$

Compute the time derivative of $V$:

$$\dot{V}(\boldsymbol{\eta}) = -\boldsymbol{\eta}^{\mathrm{T}} \boldsymbol{\Lambda} \boldsymbol{\eta} - 2\gamma \boldsymbol{\eta}^{\mathrm{T}} \hat{\boldsymbol{L}} \boldsymbol{\eta} + 2 \sum_{i=1}^{N} \boldsymbol{\eta}_i^{\mathrm{T}} \boldsymbol{P}_i^{-1} \boldsymbol{\Gamma}_i \boldsymbol{\omega}_i. \tag{8}$$

With Assumption 1, one obtains

$$\dot{V}(\boldsymbol{\eta}) \leq -\delta \|\boldsymbol{\eta}\|^2 + 2 \frac{1}{\underline{p}} \boldsymbol{\eta}^{\mathrm{T}} \boldsymbol{\Gamma} \tilde{\boldsymbol{\omega}}, \tag{9}$$

where $\boldsymbol{\Gamma} = \mathrm{diag}(\boldsymbol{\Gamma}_i)$ and $\tilde{\boldsymbol{\omega}} = \mathrm{col}(\boldsymbol{\omega}_i)$. Furthermore,

$$\begin{aligned} \dot{V}(\boldsymbol{\eta}) \leq & -\delta \|\boldsymbol{\eta}\|^2 + \frac{1}{\underline{p}} b \|\boldsymbol{\eta}\|^2 + \frac{1}{\underline{p} b} \|\boldsymbol{\Gamma} \tilde{\boldsymbol{\omega}}\|^2 \\ \leq & -\left( \delta \underline{p} - \frac{1}{\underline{p}} b \overline{p} \right) V(\boldsymbol{\eta}) + \frac{1}{\underline{p} b} \|\boldsymbol{\Gamma} \tilde{\boldsymbol{\omega}}\|^2. \end{aligned}$$

Choosing $b > 0$, $\delta \underline{p} - \frac{1}{\underline{p}} b \overline{p} > 0$, and bounded $\|\boldsymbol{\Gamma} \tilde{\boldsymbol{\omega}}\|$, we obtain that $\boldsymbol{\eta}$ is bounded.

**Remark 1** Assume $\boldsymbol{\Lambda} + 2\gamma \hat{\boldsymbol{L}} \geq \delta \boldsymbol{I}$ in Assumption 1; i.e., $\boldsymbol{\Lambda} + 2\gamma \hat{\boldsymbol{L}}$ is positive definite. $\hat{\boldsymbol{L}}$ is positive semidefinite. The dimension of the input noise or the dimension of the measurement should be equal to the dimension of the states to make sure that $\boldsymbol{\Lambda}$ is positive definite.

If the network is connected, $\boldsymbol{\eta}^{\mathrm{T}} \hat{\boldsymbol{L}} \boldsymbol{\eta} = 0$ only when $\boldsymbol{\eta} = \boldsymbol{0}$ or $\boldsymbol{\eta}_1 = \boldsymbol{\eta}_2 = \ldots = \boldsymbol{\eta}_N$. It is very rare that all the estimation errors are equal. When it happens, one obtains

$$\boldsymbol{\eta}^{\mathrm{T}} \boldsymbol{\Lambda} \boldsymbol{\eta} = \boldsymbol{\eta}_1^{\mathrm{T}} \left[ \sum_i (\boldsymbol{H}_i^{\mathrm{T}} \boldsymbol{R}_i^{-1} \boldsymbol{H}_i + \boldsymbol{P}_i^{-1} \boldsymbol{B} \boldsymbol{Q} \boldsymbol{B}^{\mathrm{T}} \boldsymbol{P}_i^{-1}) \right] \boldsymbol{\eta}_1.$$

Thus, if the summation is positive definite, $\boldsymbol{\Lambda} + 2\gamma \hat{\boldsymbol{L}}$ would also be positive definite, which is more possible in the cases with heterogeneous sensors.

## 4 Kinematic model of unmanned aerial vehicles

Consider a team of $N$ UAVs tracking a mobile target. Assume that the UAVs are flying at a constant height. The dynamics of the $i^{\mathrm{th}}$ UAV is given by

$$\begin{cases} q_{i,x} = p_{i,\mathrm{v}} \cos \theta_i, \\ q_{i,y} = p_{i,\mathrm{v}} \sin \theta_i, \\ \dot{p}_{i,\mathrm{v}} = a_i, \\ \dot{\theta}_i = w_i, \end{cases} \tag{10}$$

where $[q_{i,x},\ q_{i,y}]$ is the position of the $i^{\mathrm{th}}$ UAV, $p_{i,\mathrm{v}}$ and $\theta_i$ are the velocity and heading of the $i^{\mathrm{th}}$ UAV respectively, and $a_i$ and $w_i$ are the control inputs. The velocity and control inputs are constrained by the capabilities of the UAVs. It is assumed that

$$\begin{cases} p_{\mathrm{v,min}} \leq p_{i,\mathrm{v}} \leq p_{\mathrm{v,max}}, \\ a_{\mathrm{min}} \leq a_i \leq a_{\mathrm{max}}, \\ w_{\mathrm{min}} \leq w_i \leq w_{\mathrm{max}}. \end{cases}$$

Defining $\boldsymbol{q}_i = [q_{i,x},\ q_{i,y}]^{\mathrm{T}}$ and $\boldsymbol{p}_i = [p_{i,x},\ p_{i,y}]^{\mathrm{T}} = [p_{i,\mathrm{v}} \cos \theta_i,\ p_{i,\mathrm{v}} \sin \theta_i]^{\mathrm{T}}$, we obtain (Oriolo et al., 2002)

$$\begin{aligned} \ddot{\boldsymbol{q}}_i = & \dot{\boldsymbol{p}}_i \\ = & \begin{pmatrix} \cos \theta_i & -p_{i,\mathrm{v}} \sin \theta_i \\ \sin \theta_i & p_{i,\mathrm{v}} \cos \theta_i \end{pmatrix} \begin{pmatrix} a_i \\ \omega_i \end{pmatrix} \\ = & \begin{pmatrix} u_{i,x} \\ u_{i,y} \end{pmatrix}, \end{aligned} \tag{11}$$

where

$$\begin{cases} a_i = u_{i,x} \cos \theta_i + u_{i,y} \sin \theta_i, \\ w_i = \dfrac{u_{i,y} \cos \theta_i - u_{i,x} \sin \theta_i}{p_{i,\mathrm{v}}}. \end{cases} \tag{12}$$

The input $w_i$ is singular if $p_{i,\mathrm{v}} = 0$, and this will never occur while the $i^{\mathrm{th}}$ UAV is moving. The equivalent linear system of Eq. (10) is given as

$$\begin{cases} \dot{\boldsymbol{q}}_i = \boldsymbol{p}_i, \\ \dot{\boldsymbol{p}}_i = \boldsymbol{u}_i, \end{cases} \tag{13}$$

where $\boldsymbol{u}_i = [u_{i,x},\ u_{i,y}]^{\mathrm{T}}$, $\boldsymbol{q}_i,\ \boldsymbol{p}_i,\ \boldsymbol{u}_i \in \mathbb{R}^2$. We further design the control input $\boldsymbol{u}_i$ for the linear system (13).

## 5 Motion control design of unmanned aerial vehicles

Since norm $\|\boldsymbol{z}\|$ is not differentiable at $\boldsymbol{z} = \boldsymbol{0}$, the $\sigma$-norm was introduced by Olfati-Saber (2006) to derive the smooth controller:

$$\|\boldsymbol{z}\|_\sigma = \frac{1}{\varepsilon} \left( \sqrt{1 + \varepsilon \|\boldsymbol{z}\|^2} - 1 \right),$$

where $\varepsilon > 0$ is a constant. The $\sigma$-norm is differentiable everywhere. The gradient of $\|\boldsymbol{z}\|_\sigma$ is given by (Olfati-Saber, 2006)

$$\sigma_\varepsilon(\boldsymbol{z}) = \nabla\|\boldsymbol{z}\|_\sigma = \frac{\boldsymbol{z}}{\sqrt{1+\varepsilon\|\boldsymbol{z}\|^2}}.$$

For the sake of collision avoidance and connectivity maintenance, repulsive and attractive actions of UAVs are needed. Let $r$, $r_a$, $r_c$, and $R$ denote the safety distance, repulsive distance, attractive distance, and communication range, respectively, where $0 < r < r_a < r_c < R$. Two bounded continuous functions $\phi_a$, $\phi_c$: $\mathbb{R}_{\geq 0} \to \mathbb{R}$ are defined to represent the repulsive and attractive forces respectively (Wang L et al., 2015):

$$\phi_a(z)\begin{cases} =0,\ z\in\big[0,\|r\|_\sigma\big]\cup\big[\|r_a\|_\sigma,+\infty\big), \\ <0,\ z\in\big(\|r\|_\sigma,\|r_a\|_\sigma\big), \end{cases} \tag{14a}$$

$$\phi_c(z)\begin{cases} =0,\ z\in\big[0,\|r_c\|_\sigma\big]\cup\big[\|R\|_\sigma,+\infty\big), \\ >0,\ z\in\big(\|r_c\|_\sigma,\|R\|_\sigma\big). \end{cases} \tag{14b}$$

The potential function is given as

$$\varphi_a(h) = \int_{\|r_a\|_\sigma}^{h} \phi_a(z)\mathrm{d}z.$$

We obtain

$$0 \leq \varphi_a(h) \leq \varphi_a(\|r\|_\sigma),\ 0 \leq \varphi_c(h) \leq \varphi_c(\|R\|_\sigma).$$

Taking into account the object of target tracking, initial link maintenance, and collision avoidance, we design the following UAV motion controller (Olfati-Saber, 2006; Wang L et al., 2015):

$$\begin{aligned} \boldsymbol{u}_i =& \sum_{j\in N_i}\phi_a\big(\|\boldsymbol{q}_j-\boldsymbol{q}_i\|_\sigma\big)\sigma_\varepsilon\big(\boldsymbol{q}_j-\boldsymbol{q}_i\big) \\ &+\sum_{j\in N_i\cap N_i^0}\phi_c\big(\|\boldsymbol{q}_j-\boldsymbol{q}_i\|_\sigma\big)\sigma_\varepsilon(\boldsymbol{q}_j-\boldsymbol{q}_i) \\ &+b_i\mathrm{sgn}\Bigg(\sum_{j\in N_i\cap N_i^0}\boldsymbol{p}_j-\boldsymbol{p}_i\Bigg)+\hat{\boldsymbol{f}}_i^\xi, \end{aligned} \tag{15}$$

where

$$\hat{\boldsymbol{f}}_i^\xi = -c_1(\boldsymbol{q}_i-\hat{\boldsymbol{q}}_{i,\xi})-c_2(\boldsymbol{p}_i-\hat{\boldsymbol{p}}_{i,\xi}). \tag{16}$$

In Eq. (15), $N_i^0$ denotes the set of neighbors of the $i^{\text{th}}$ UAV at the beginning, $N_i$ denotes the set of neighbors of the $i^{\text{th}}$ UAV at the current time, $b_i$ is a positive constant, and $\mathrm{sgn}(\cdot)$ is the signum function satisfying

$$\mathrm{sgn}(z) = \begin{cases} 1,\ z>0, \\ 0,\ z=0, \\ -1,\ z<0. \end{cases}$$

$\hat{\boldsymbol{f}}_i^\xi$ is for target tracking, which drives the $i^{\text{th}}$ UAV to move toward the target, improving the accuracy of target estimation. In Eq. (16), $\hat{\boldsymbol{q}}_{i,\xi}$ and $\hat{\boldsymbol{p}}_{i,\xi}$ are the estimated target position and velocity respectively obtained by the $i^{\text{th}}$ UAV using the estimation algorithm in Eqs. (3)–(5). $c_1 > 0$ and $c_2 > 0$ are the feedback gains. Clearly, the UAV motion control and target state estimation are coupled.

## 6 Analysis of the coupled system

Let $\boldsymbol{q}_\xi$ and $\boldsymbol{p}_\xi$ denote the position and velocity of the target, respectively. Then Eq. (16) can be rewritten as

$$\begin{aligned} \hat{\boldsymbol{f}}_i^\xi =& -c_1(\boldsymbol{q}_i-\boldsymbol{q}_\xi+\boldsymbol{q}_\xi-\hat{\boldsymbol{q}}_{i,\xi}) \\ &-c_2(\boldsymbol{p}_i-\boldsymbol{p}_\xi+\boldsymbol{p}_\xi-\hat{\boldsymbol{p}}_{i,\xi}) \\ =&\boldsymbol{f}_i^\xi-\boldsymbol{C}\boldsymbol{\eta}_i, \end{aligned}$$

where $\boldsymbol{f}_i^\xi = -c_1(\boldsymbol{q}_i-\boldsymbol{q}_\xi)-c_2(\boldsymbol{p}_i-\boldsymbol{p}_\xi)$, $\boldsymbol{C} = [c_1\boldsymbol{I}_m,\ c_2\boldsymbol{I}_m]$, and $\boldsymbol{\eta}_i = [(\boldsymbol{q}_\xi-\hat{\boldsymbol{q}}_{i,\xi})^{\mathrm{T}},\ (\boldsymbol{p}_\xi-\hat{\boldsymbol{p}}_{i,\xi})^{\mathrm{T}}]^{\mathrm{T}}$ is the estimation error. If Assumption 1 holds, the estimation error $\boldsymbol{\eta}_i$ is bounded, and there exists a constant $b' > 0$ satisfying $\|\boldsymbol{C}\boldsymbol{\eta}_i\| < b'$.

The controller described in Eq. (15) depends on the initial states of the UAVs. Define the collective potential function as

$$\begin{aligned} V(\boldsymbol{q},\boldsymbol{q}_0) =& \frac{1}{2}\sum_i\sum_{j\in N_i}\varphi_a\big(\|\boldsymbol{q}_j-\boldsymbol{q}_i\|_\sigma\big) \\ &+\frac{1}{2}\sum_i\sum_{j\in N_i\cap N_i^0}\varphi_c\big(\|\boldsymbol{q}_j-\boldsymbol{q}_i\|_\sigma\big). \end{aligned}$$

The dynamics of the $i^{\text{th}}$ UAV can be expressed as

$$\begin{cases} \dot{\boldsymbol{q}}_i =\boldsymbol{p}_i, \\ \dot{\boldsymbol{p}}_i =-\nabla_{\boldsymbol{q}_i}V(\boldsymbol{q},\boldsymbol{q}_0)+b_i\mathrm{sgn}\Bigg(\sum_{j\in N_i\cap N_i^0}(\boldsymbol{p}_j-\boldsymbol{p}_i)\Bigg) \\ \qquad\quad +\boldsymbol{f}_i^\xi-\boldsymbol{C}\boldsymbol{\eta}_i. \end{cases} \tag{17}$$

Let $\boldsymbol{q}_{\mathrm{c}} = \dfrac{1}{N}\sum\limits_{i=1}^{N}\boldsymbol{q}_i$ and $\boldsymbol{p}_{\mathrm{c}} = \dfrac{1}{N}\sum\limits_{i=1}^{N}\boldsymbol{p}_i$ be the position and velocity center of the UAV group, respectively. The relative position and velocity of the

$i^{\text{th}}$ UAV are given as $\boldsymbol{x}_i = \boldsymbol{q}_i - \boldsymbol{q}_{\text{c}}$ and $\boldsymbol{v}_i = \boldsymbol{p}_i - \boldsymbol{p}_{\text{c}}$, respectively. We have $\boldsymbol{x}_i - \boldsymbol{x}_j = \boldsymbol{q}_i - \boldsymbol{q}_j$, $\boldsymbol{v}_i - \boldsymbol{v}_j = \boldsymbol{p}_i - \boldsymbol{p}_j$, $\sum\limits_i \boldsymbol{x}_i = \boldsymbol{0}$, and $\sum\limits_i \boldsymbol{v}_i = \boldsymbol{0}$.

Consider the target dynamics and sensor measurement model in Eqs. (1) and (2), and the linear kinematic model and distributed controller in Eqs. (13) and (15). Each UAV adopts the distributed Kalman consensus filter in Eqs. (3)–(5) for target state estimation. Define the target state estimation of the UAV network as $\Sigma_{\text{e}}$, the collective UAV motion dynamics as $\Sigma_{\text{c}}$, and the coupled system as $\Sigma$.

Since the feedback term $\hat{\boldsymbol{f}}_i^{\xi}$ in Eq. (15) is linear, according to Lemma 2 in Olfati-Saber (2006), we have the following proposition (Olfati-Saber and Jalalkamali, 2012):

**Proposition 2** $\Sigma_{\text{c}}$ can be separated into subsystems which consist of the dynamics of UAVs relative to the group center ($\Sigma_{\text{s}}$) and the translational dynamics of the UAV group center ($\Sigma_{\text{t}}$); i.e., the coupled system $\Sigma$ is an integration of translational dynamics, relative dynamics of UAVs, and collective estimation dynamics:

$$\Sigma_{\text{s}}: \begin{cases} \dot{\boldsymbol{x}}_i = \boldsymbol{v}_i, \\ \dot{\boldsymbol{v}}_i = -\nabla_{\boldsymbol{x}_i} V(\boldsymbol{x}, \boldsymbol{x}_0) \\ \qquad\quad + b_i \text{sgn}\Big(\sum\limits_{j\in N_i\cap N_i^0} (\boldsymbol{v}_j - \boldsymbol{v}_i)\Big) \\ \qquad\quad - c_1\boldsymbol{x}_i - c_2\boldsymbol{v}_i + \boldsymbol{\delta}_i - \bar{\boldsymbol{\delta}}, \end{cases}$$

$$\Sigma_{\text{t}}: \begin{cases} \dot{\boldsymbol{q}}_{\text{c}} = \boldsymbol{p}_{\text{c}}, \\ \dot{\boldsymbol{p}}_{\text{c}} = -c_1(\boldsymbol{q}_{\text{c}} - \boldsymbol{q}_\xi) - c_2(\boldsymbol{p}_{\text{c}} - \boldsymbol{p}_\xi) + \bar{\boldsymbol{\delta}}, \end{cases}$$

$$\Sigma_{\text{e}}: \dot{\boldsymbol{\eta}}_i = \boldsymbol{F}_i\boldsymbol{\eta}_i + \gamma\boldsymbol{P}_i \sum_{j\in N_i} (\boldsymbol{\eta}_j - \boldsymbol{\eta}_i) + \boldsymbol{\Gamma}_i\boldsymbol{\omega}_i,$$

where $\boldsymbol{\delta}_i = -\boldsymbol{C}\boldsymbol{\eta}_i$ and $\bar{\boldsymbol{\delta}} = \dfrac{1}{N}\sum\limits_i \boldsymbol{\delta}_i$.

Let $\boldsymbol{q}_0$ and $\boldsymbol{p}_0$ be the initial position and velocity of the UAV network, respectively, and $G_0$ be the initial proximity graph. The corresponding initial relative states are given by $\boldsymbol{x}_0$ and $\boldsymbol{v}_0$. Define the energy function of system $\Sigma_{\text{s}}$ as

$$H(\boldsymbol{x}_0, \boldsymbol{x}, \boldsymbol{v}) = V(\boldsymbol{x}, \boldsymbol{x}_0) + \frac{1}{2}\|\boldsymbol{x}\|^2 + \frac{1}{2}\|\boldsymbol{v}\|^2.$$

Since system $\Sigma_{\text{s}}$ depends on the initial states, the invariant set theory may not be efficient. Define the admissible set as (Wang L et al., 2015)

$$\Omega = \Big\{(\boldsymbol{x}, \boldsymbol{v}) : H(\boldsymbol{x}_0, \boldsymbol{x}, \boldsymbol{v}) < c^*, \\ c^* = \min(\varphi_a(\|r\|_\sigma),\ \varphi_c(\|R\|_\sigma)),\ \sum_i \boldsymbol{x}_i = \boldsymbol{0}, \\ \sum_i \boldsymbol{v}_i = \boldsymbol{0},\ \boldsymbol{x}_i \neq \boldsymbol{x}_j \text{ for } i \neq j\Big\}.$$

**Proposition 3** Given the initial UAV states $(\boldsymbol{q}_0, \boldsymbol{p}_0)$, the corresponding relative states are denoted as $(\boldsymbol{x}_0, \boldsymbol{v}_0)$. If (1) $(\boldsymbol{x}_0, \boldsymbol{v}_0) \in \Omega$, (2) the initial proximity graph $G_0$ is complete, (3) Assumption 1 holds, and (4) the constant $b_i$ in Eq. (15) satisfies $b_i > 2b'$, then the initial communication links are maintained and the inter-UAV distances are always larger than the safety distance.

**Proposition 4** For a mobile target with bounded acceleration inputs, the deviation between the states of the group center and the target is bounded; i.e., the group would keep pace with the target. The deviation is also related to the estimation errors and the acceleration input of the target.

Proofs of Propositions 3 and 4 are given in the Appendix.

## 7 Simulation results

Consider a target moving in a two-dimensional (2D) space with the discrete-time kinematic model:

$$\boldsymbol{x}(k+1) = \boldsymbol{A}x(k) + \boldsymbol{B}\boldsymbol{\omega}(k),$$

where $\boldsymbol{x} = [\boldsymbol{q}_\xi^{\text{T}},\ \boldsymbol{p}_\xi^{\text{T}}]^{\text{T}}$, $\boldsymbol{A} = \begin{bmatrix} \boldsymbol{I}_2 & T\boldsymbol{I}_2 \\ \boldsymbol{0} & \boldsymbol{I}_2 \end{bmatrix}$, $\boldsymbol{B} = \begin{bmatrix} (T^2/2)\boldsymbol{I}_2 \\ \boldsymbol{I}_2 \end{bmatrix}$, and $T = 0.1$ s is the time step.

The sensing model of the $i^{\text{th}}$ UAV is given by

$$\boldsymbol{z}_i(k) = \boldsymbol{H}_i\boldsymbol{x}(k) + \boldsymbol{v}_i(k),$$

where

$$\boldsymbol{H}_i = [\boldsymbol{I}_2,\ \boldsymbol{0}].$$

Here, $\boldsymbol{\omega}(k)$ and $\boldsymbol{v}_i(k)$ are zero-mean Gaussian noise with statistics:

$$\begin{cases} E\left[\boldsymbol{\omega}(k)\boldsymbol{\omega}^{\text{T}}(l)\right] = \boldsymbol{Q}_k\delta_{kl}, \\ E\left[\boldsymbol{v}_i(k)\boldsymbol{v}_i^{\text{T}}(l)\right] = \boldsymbol{R}_{i,k}\delta_{kl}. \end{cases}$$

Without loss of generality, assume that the measurement errors are related to the distance between the $i^{\text{th}}$ UAV and the target; hence,

$$\boldsymbol{R}_i = (\alpha(d_i - r_{\text{s}})^2 + \sigma_0^2)\boldsymbol{I}_2,$$

where $\alpha$, $r_{\text{s}}$, and $\sigma_0$ are positive constants, and $d_i$ is the distance between the $i^{\text{th}}$ UAV and the target. We can see that $\boldsymbol{R}_i$ reaches its minimum if $d_i = r_{\text{s}}$.

The functions $\phi_a$ and $\phi_c$ in Eq. (14) are defined as (Wang L et al., 2015)

$$\phi_a(z) = \begin{cases} 0, \ z \in [0, \|r\|_\sigma] \cup [\|r_a\|_\sigma, +\infty), \\ -\alpha_1 \sin\left(\dfrac{z - \|r\|_\sigma}{\|r_a\|_\sigma - \|r\|_\sigma}\pi\right), \\ \quad z \in (\|r\|_\sigma, \|r_a\|_\sigma), \end{cases}$$

$$\phi_c(z) = \begin{cases} 0, \ z \in [0, \|r_c\|_\sigma] \cup [\|R\|_\sigma, +\infty), \\ \alpha_2 \sin\left(\dfrac{z - \|r_c\|_\sigma}{\|R\|_\sigma - \|r_c\|_\sigma}\pi\right), \\ \quad z \in (\|r_c\|_\sigma, \|R\|_\sigma), \end{cases}$$

where the constants are chosen as $\alpha_1 = \alpha_2 = 20$.

**Example 1** Consider a network of four UAVs tracking a mobile target cooperatively. The initial position of the target is (600, 600) m, and the initial positions of the UAVs are (200, 200), (400, 200), (400, 400), and (200, 400) m. The communication range and safety distance between UAVs are $R$=350 m and $r$=50 m, respectively. The initial proximity graph $G_0$ is complete.

The acceleration and changing rate of the heading angle of the $i^{\text{th}}$ UAV are computed from Eq. (12). The control input constraints are given as [−5, 5] m/s$^2$ and [−0.3, 0.3] rad/s. The velocity of the UAVs is constrained within [20, 30] m/s. The initial velocities and heading angles of the UAVs are all set as 21 m/s and 0.79 rad, respectively. The initial velocity of the target is $\boldsymbol{p}_\xi = [15, 10]^{\text{T}}$ m/s, and the acceleration input of the target satisfies $\boldsymbol{u}_\xi \sim N(0, 5^2\boldsymbol{I}_2)$. Parameters of estimation are given as $\boldsymbol{Q} = 100\boldsymbol{I}_2$, $\alpha = 0.003$, $r_{\text{s}} = 150$ m, $\sigma_0 = 10$, and $\boldsymbol{P}_0 = \text{diag}(500, 500, 50, 50)$.

Figs. 1–4 show the numerical results of Example 1. The trajectories of the target, UAVs, and the center of the UAV group are presented in Fig. 1. It can be seen that the UAVs move toward the target cooperatively. The distance between each UAV can be found in Fig. 2. It shows that the distances between the initially connected UAVs are smaller than the communication range $R$. The distances between any two UAVs are larger than the safety distance $r$. The target trajectory and the estimated trajectories of the four UAVs are presented in Fig. 3. The mean of norm of estimation errors, $\sum_i \|\boldsymbol{\eta}_i\|/N$, is given in Fig. 4. It can be seen that the estimation errors

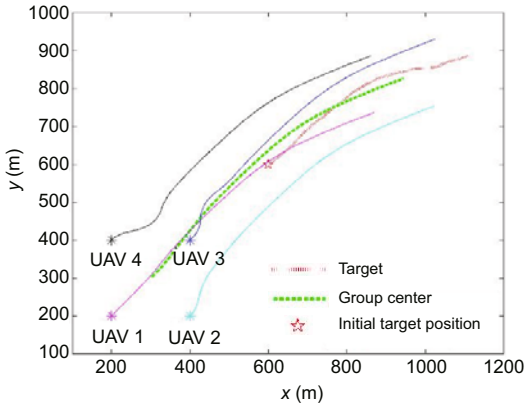


**Fig. 1 Trajectories of the target and UAVs in Example 1**

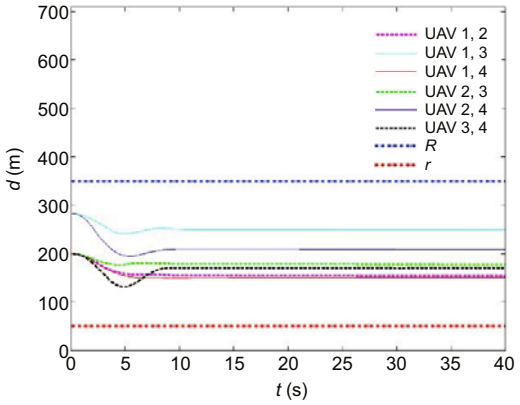


**Fig. 2 Inter-UAV distances in Example 1**

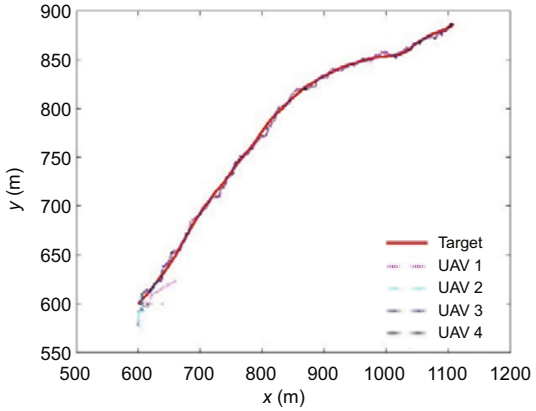


**Fig. 3 Target trajectory and estimated trajectories of the four UAVs in Example 1**

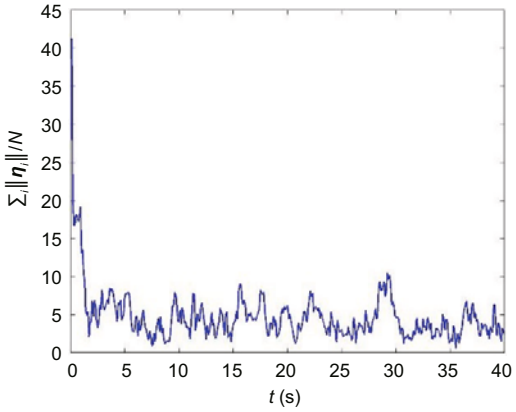


**Fig. 4 Mean of norm of the estimation errors in Example 1**

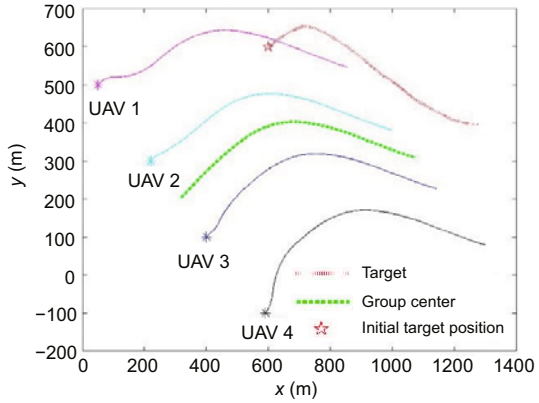


**Fig. 5 Trajectories of the target and UAVs in Example 2**

converge within 10 s after 3 s and that the target tracking can be accomplished.

**Example 2** The assumption that the initial proximity graph is complete in Proposition 3 is a little conservative here. In the simulations, we consider the case in which the UAVs are arranged in a line so that each UAV can communicate with only its immediate neighbors. The initial positions of the UAVs are (50, 500), (220, 300), (400, 100), and (590, −100) m. Other parameters are the same as in Example 1.

Figs. 5–8 show the numerical results of Example 2. The trajectories of the target, UAVs, and the center of the UAV group are presented in Fig. 5. The distance between each UAV can be found in Fig. 6. It shows that the connectivity preservation and collision avoidance constraints are all satisfied. The target trajectory and estimated trajectories of the four UAVs and the mean of the norm of the estimation errors are presented in Figs. 7 and 8, respectively.

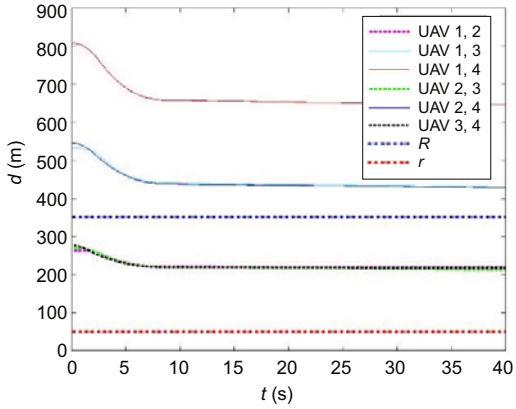


**Fig. 6 Inter-UAV distances in Example 2. Dashed lines represent that there exist initial communication links between UAVs, while solid lines represent that there do not exist initial communication links between UAVs**

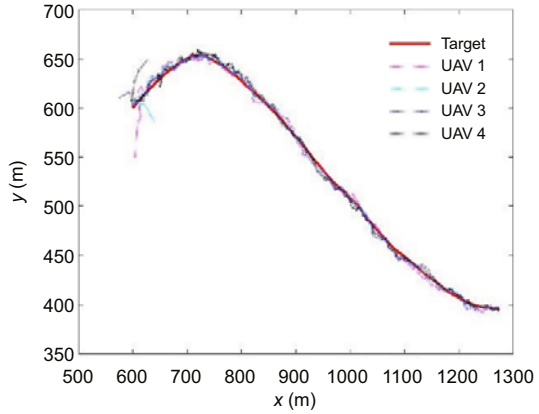


**Fig. 7 Target trajectory and estimated trajectories of the four UAVs in Example 2**

## 8 Conclusions

The distributed Kalman consensus filter has been presented, and the boundedness of estimation errors has also been analyzed. The kinematic model of UAVs has been linearized, and the distributed potential-based UAV motion controller for target tracking, connectivity maintenance, and collision avoidance has been designed. The analysis of the multi-UAV target tracking system which integrates estimation and motion control showed that the network connectivity and collision avoidance can be guaranteed, and that the estimation errors would converge. For a mobile target with bounded noise as acceleration input, the group of UAVs would track the target stably. Numerical simulations demonstrated the validity of the proposed method.

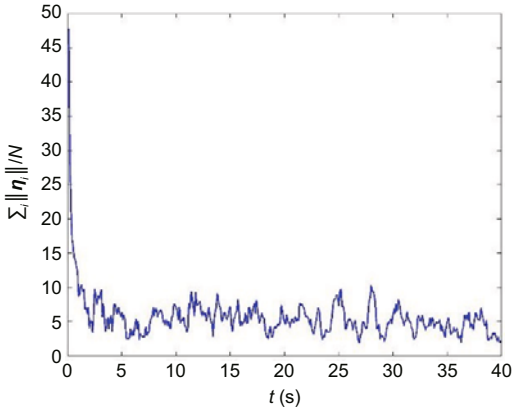


**Fig. 8 Mean of norm of the estimation errors in Example 2**

## Contributors

Rui ZHOU and Bin DI designed the research and processed the data. Bin DI and Yu FENG drafted the manuscript. Rui ZHOU and Jiang ZHAO helped organize the manuscript. Yu FENG, Jiang ZHAO, and Yan HU revised and finalized the paper.

## Compliance with ethics guidelines

Rui ZHOU, Yu FENG, Bin DI, Jiang ZHAO, and Yan HU declare that they have no conflict of interest.

## References

Ajorlou A, Momeni A, Aghdam AG, 2010. A class of bounded distributed control strategies for connectivity preservation in multi-agent systems. *IEEE Trans Autom Contr*, 55(12):2828-2833. https://doi.org/10.1109/TAC.2010.2072570

Casbeer DW, Beard R, 2009a. Distributed information filtering using consensus filters. American Control Conf, p.1882-1887. https://doi.org/10.1109/ACC.2009.5160531

Casbeer DW, Beard R, 2009b. Multi-static radar target tracking using information consensus filters. AIAA Guidance, Navigation, and Control Conf, p.1-9. https://doi.org/10.2514/6.2009-6223

Godsil C, Royle G, 2001. Algebraic Graph Theory. Springer-Verlag, New York, USA. https://doi.org/10.1007/978-1-4613-0163-9

Ji M, Egerstedt M, 2007. Distributed coordination control of multiagent systems while preserving connectedness. *IEEE Trans Robot*, 23(4):693-703. https://doi.org/10.1109/TRO.2007.900638

Kan Z, Dani AP, Shea JM, et al., 2012. Network connectivity preserving formation stabilization and obstacle avoidance via a decentralized controller. *IEEE Trans Autom Contr*, 57(7):1827-1832. https://doi.org/10.1109/TAC.2011.2178883

Kim Y, Mesbahi M, 2006. On maximizing the second smallest eigenvalue of a state-dependent graph Laplacian. *IEEE Trans Autom Contr*, 51(1):116-120. https://doi.org/10.1109/TAC.2005.861710

Kim Y, Gu DW, Postlethwaite I, 2010. Robust target tracking using distributed unmanned aerial vehicle networks. *Proc Inst Mech Eng Part G J Aerosp Eng*, 224(4):417-426. https://doi.org/10.1243/09544100JAERO578

Li TC, Fan HQ, García J, et al., 2019. Second-order statistics analysis and comparison between arithmetic and geometric average fusion: application to multi-sensor target tracking. *Inform Fus*, 51:233-243. https://doi.org/10.1016/j.inffus.2019.02.009

Lim S, Kim Y, Lee D, et al., 2013. Standoff target tracking using a vector field for multiple unmanned aircrafts. *J Intell Robot Syst*, 69(1-4):347-360. https://doi.org/10.1007/s10846-012-9765-7

Liu QY, Wang ZD, He X, et al., 2018. On Kalman-consensus filtering with random link failures over sensor networks. *IEEE Trans Autom Contr*, 63(8):2701-2708. https://doi.org/10.1109/TAC.2017.2774601

Liu S, Zhang HM, 2011. Optimal Estimation Theory. Science Press, Beijing (in Chinese).

Ma LL, Hovakimyan N, 2013. Cooperative target tracking in balanced circular formation: multiple UAVs tracking a ground vehicle. American Control Conf, p.5386-5391. https://doi.org/10.1109/ACC.2013.6580679

Olfati-Saber R, 2006. Flocking for multi-agent dynamic systems: algorithms and theory. *IEEE Trans Autom Contr*, 51(3):401-420. https://doi.org/10.1109/TAC.2005.864190

Olfati-Saber R, 2007a. Distributed Kalman filtering for sensor networks. Proc 46th IEEE Conf on Decision and Control, p.12-14. https://doi.org/10.1109/CDC.2007.4434303

Olfati-Saber R, 2007b. Distributed tracking for mobile sensor networks with information-driven mobility. American Control Conf, p.728-734. https://doi.org/10.1109/ACC.2007.4282261

Olfati-Saber R, 2009. Kalman-consensus filter: optimality, stability, and performance. Proc 48th IEEE Conf on Decision and Control held jointly with 28th Chinese Control Conf, p.7036-7042. https://doi.org/10.1109/CDC.2009.5399678

Olfati-Saber R, Jalalkamali P, 2012. Coupled distributed estimation and control for mobile sensor networks. *IEEE Trans Autom Contr*, 57(10):2609-2614. https://doi.org/10.1109/TAC.2012.2190184

Oriolo G, de Luca A, Vendittelli M, 2002. WMR control via dynamic feedback linearization: design, implementation, and experimental validation. *IEEE Trans Contr Syst Technol*, 10(6):835-852. https://doi.org/10.1109/TCST.2002.804116

Stachura M, Frew EW, 2011. Cooperative target localization with a communication-aware unmanned aircraft system. *J Guid Contr Dynam*, 34(5):1352-1362. https://doi.org/10.2514/1.51591

Tanner HG, Jadbabaie A, Pappas GJ, 2007. Flocking in fixed and switching networks. *IEEE Trans Autom Contr*, 52(5):863-868. https://doi.org/10.1109/TAC.2007.895948

Wang L, Wang XF, Hu XM, 2015. Connectivity maintenance and distributed tracking for double-integrator agents with bounded potential functions. *Int J Robust Nonl Contr*, 25(4):542-588. https://doi.org/10.1002/rnc.3105

Wang YT, Li JB, Sun Q, 2013. Coordinated target tracking by distributed unscented information filter in sensor networks with measurement constraints. *Math Probl Eng*, 2013:402732.
https://doi.org/10.1155/2013/402732

Wen G, Duan Z, Su H, et al., 2012. A connectivity-preserving flocking algorithm for multi-agent dynamical systems with bounded potential function. *IET Contr Theory Appl*, 6(6):813-821.
https://doi.org/10.1049/iet-cta.2011.0532

Yan MD, Zhu X, Zhang XX, et al., 2017. Consensus-based three-dimensional multi-UAV formation control strategy with high precision. *Front Inform Technol Electron Eng*, 18(7):968-977.
https://doi.org/10.1631/FITEE.1600004

Yang P, Freeman RA, Gordon GJ, et al., 2010. Decentralized estimation and control of graph connectivity for mobile sensor networks. *Automatica*, 46(2):390-396.
https://doi.org/10.1016/j.automatica.2009.11.012

Yu ZQ, Liu ZX, Zhang YM, et al., 2019. Decentralized fault-tolerant cooperative control of multiple UAVs with prescribed attitude synchronization tracking performance under directed communication topology. *Front Inform Technol Electron Eng*, 20(5):685-700.
https://doi.org/10.1631/FITEE.1800569

Zavlanos MM, Pappas GJ, 2007. Potential fields for maintaining connectivity of mobile networks. *IEEE Trans Robot*, 23(4):812-816.
https://doi.org/10.1109/TRO.2007.900642

Zavlanos MM, Pappas GJ, 2008. Distributed connectivity control of mobile networks. *IEEE Trans Robot*, 24(6):1416-1428.
https://doi.org/10.1109/TRO.2008.2006233

Zavlanos MM, Tanner HG, Jadbabaie A, et al., 2009. Hybrid control for connectivity preserving flocking. *IEEE Trans Autom Contr*, 54(12):2869-2875.
https://doi.org/10.1109/TAC.2009.2033750

Zavlanos MM, Egerstedt MB, Pappas GJ, 2011. Graph-theoretic connectivity control of mobile robot networks. *Proc IEEE*, 99(9):1525-1540.
https://doi.org/10.1109/JPROC.2011.2157884

## Appendix: Proofs of Propositions 3 and 4

**Proof of Proposition 3** Given $(\boldsymbol{x}_0, \boldsymbol{v}_0) \in \Omega$, we assume that

$$H(\boldsymbol{x}_0, \boldsymbol{x}_0, \boldsymbol{v}) = c'.$$

Since $c' < c^* = \min(\varphi_a(\|r\|_\sigma),\ \varphi_c(\|R\|_\sigma))$, there exists a constant $\gamma' > 0$ such that $H(\boldsymbol{x}_0, \boldsymbol{x}, \boldsymbol{v}) > c'$ for any $(x, v)$ in the set

$$\begin{aligned}\big\{(\boldsymbol{x},\boldsymbol{v}) : &\exists i \neq j \text{ such that}\\ &r < \|\boldsymbol{x}_i - \boldsymbol{x}_j\| < r + \gamma'(R-r)\\ &\text{or } \exists (k,l) \in E(G_0) \text{ such that}\\ &r + (1-\gamma')(R-r) < \|\boldsymbol{x}_k - \boldsymbol{x}_l\| < R\big\}.\end{aligned}$$

For any $(\boldsymbol{x}_0, \boldsymbol{v}_0) \in \Omega$, define the following compact set:

$$\begin{aligned}\Psi(G_0,\gamma',c') = \Big\{&(\boldsymbol{x},\boldsymbol{v}) : H(\boldsymbol{x}_0,\boldsymbol{x},\boldsymbol{v}) \le c',\\ &\sum_i \boldsymbol{x}_i = \boldsymbol{0},\ \sum_i \boldsymbol{v}_i = \boldsymbol{0}, \|\boldsymbol{x}_i - \boldsymbol{x}_j\| \ge r + \gamma'(R-r)\\ &\text{for } i \neq j,\ \|\boldsymbol{x}_k - \boldsymbol{x}_l\| \le r + (1-\gamma')(R-r)\\ &\text{for } (k,l) \in E(G_0)\Big\}.\end{aligned}$$

It is shown that if $\dot{H}(\boldsymbol{x}_0, \boldsymbol{x}, \boldsymbol{v}) \le 0$, starting with the initial state $(\boldsymbol{x}_0, \boldsymbol{v}_0) \in \Omega$, the solution of system $\Sigma_{\mathrm{s}}$ will be in the set $\Psi$ forever (Wang L et al., 2015).

It is assumed that $G_0$ is complete. We have

$$\begin{cases}\dot{\boldsymbol{x}}_i = \boldsymbol{v}_i,\\ \dot{\boldsymbol{v}}_i = -\nabla_{\boldsymbol{x}_i} V(\boldsymbol{x},\boldsymbol{x}_0) - b_i \mathrm{sgn}(\boldsymbol{v}_i) - c_1\boldsymbol{x}_i - c_2\boldsymbol{v}_i\\ \qquad\quad + \boldsymbol{\delta}_i - \bar{\boldsymbol{\delta}}.\end{cases}$$

The derivative of the energy function is given by

$$\begin{aligned}\dot{H}(\boldsymbol{x}_0,\boldsymbol{x},\boldsymbol{v}) =& -c_2\|\boldsymbol{v}\|^2 - \sum_i b_i \|\boldsymbol{v}_i\|_1 + \sum_i \boldsymbol{v}_i^{\mathrm{T}}(\boldsymbol{\delta}_i - \bar{\boldsymbol{\delta}})\\ \le& -c_2\|\boldsymbol{v}\|^2 - \sum_i \left(b_i - \left\|\boldsymbol{\delta}_i - \bar{\boldsymbol{\delta}}\right\|\right)\|\boldsymbol{v}_i\|\\ \le& 0.\end{aligned}$$

Therefore, the initial communication links are maintained and the inter-UAV distances are always larger than the safety distance.

**Proof of Proposition 4** The dynamics of the mobile target is given by

$$\begin{cases}\dot{\boldsymbol{q}}_\xi = \boldsymbol{p}_\xi,\\ \dot{\boldsymbol{p}}_\xi = \boldsymbol{u}_\xi,\end{cases}$$

where $\boldsymbol{u}_\xi$ is the bounded noise as acceleration input. Define the deviations of the state between the group center and the target as $\boldsymbol{y}_1 = \boldsymbol{q}_{\mathrm{c}} - \boldsymbol{q}_\xi$ and $\boldsymbol{y}_2 = \boldsymbol{p}_{\mathrm{c}} - \boldsymbol{p}_\xi$. The dynamics of the deviations can be written as

$$\begin{cases}\dot{\boldsymbol{y}}_1 = \boldsymbol{y}_2,\\ \dot{\boldsymbol{y}}_2 = -c_1\boldsymbol{y}_1 - c_2\boldsymbol{y}_2 + \bar{\boldsymbol{\delta}} - \boldsymbol{u}_\xi.\end{cases}$$

Choosing $c_1$ and $c_2$ to ensure the stability of the linear system, and noting that the input $\bar{\boldsymbol{\delta}} - \boldsymbol{u}_\xi$ is bounded, one obtains that the deviations are bounded.